



# Thermal fatigue behavior of Al–Si/SiC<sub>p</sub> composite synthesized by spray deposition

Li Wei, Chen Zhenhua\*, Chen Ding, Fan Cang, Wang Canrang

School of Materials Science and Engineering, Hunan University, Changsha, Hunan 410082, PR China

## ARTICLE INFO

### Article history:

Received 1 July 2009

Received in revised form 10 March 2010

Accepted 15 March 2010

Available online 19 March 2010

### Keywords:

Composite materials

Rapid solidification

Microstructure

Thermal expansion

Thermal analysis

## ABSTRACT

The thermal fatigue behavior of Al–Si/SiC<sub>p</sub> (15 vol.% SiC particulate) composite synthesized by multi-layer spray-deposition was studied for the crack initiation and propagation characteristics. Specimens containing a V-shaped notch were found to commence crack initiation at the notch tip. Samples with high micro-hardness and low porosity volume fraction show superior thermal fatigue resistance. Crack propagation rate and micro-hardness exhibit quasi-periodic up-and-down variation, while exhibiting an opposite variation, i.e. every increase of crack propagation speed corresponds to a decrease of micro-hardness. Crack propagating through the Si particles and around Si particles are observed. The cracking of SiC particles and the debonding of reinforcement/matrix are proven to be the main mechanism when the crack-tip interacts with SiC particles.

© 2010 Elsevier B.V. All rights reserved.

## 1. Introduction

SiC particle reinforced Al–Si alloy composites exhibit high strength, low thermal expansion and high wear resistance. These properties, together with the low density, make these composites very interesting for the automotive industry where they can successfully replace cast iron parts in wear applications [1,2]. However, the conventional ingot metallurgy method such as stirring casting leads to coarse primary Si phase and ceramic particle agglomeration which limit the further improvement of the properties. Spray deposition technology, an approach that combines rapid solidification and near-net-shape fabrication, can offer an effective way to produce preforms in a single-step operation directly from a molten alloy [3].

The particulate reinforced composites employed for structural components in engineering applications are often subjected to severe thermal and mechanical loads simultaneously, produced by cyclic or periodic temperature changes. Thermal load will lead to intense thermal stress concentration in the components of composites because of the mismatch of thermal and mechanical properties between the metal–matrix and ceramic reinforced particles [4,5]. Such a concentration of thermal stress around defects often results in catastrophic failure of components. Therefore, it would be necessary to understand the thermal fatigue property of such composites.

The research on the thermal fatigue behavior of metal–matrix composites (MMC) has been conducted by a few investigators. For

example, the thermal fatigue behavior of an A356/SiC<sub>p</sub> composite prepared by high-pressure infiltration cast was examined [6]. The study on Al/SiC<sub>p</sub> composite synthesized by pressureless melt infiltration was undertaken [7]. Al/C and Al/SiC continuous fiber-reinforced MMC was also studied for the interfacial damage during thermal cycling [8]. However, little research has been reported about thermal fatigue behavior of this kind of composites synthesized by spray deposition. This paper is aimed at presenting the thermal fatigue behavior of this type of composite.

## 2. Experimental procedures

### 2.1. Material

Experimental composite reinforced with 15 vol.% SiC particles was prepared by the crucible movable spray deposition technology developed by the authors, the details of which were described elsewhere [9]. The nominal chemical composition (wt.%) of the matrix alloy is Si 20, Cu 3, Mg 1, Mn 0.5, Al balance. The SiC particles have an average diameter of 15 μm. Samples with 48 mm in diameter and 150 mm in height were machined from the center of the preform. They were subjected to hot compression twice at 450 °C on a 630 tonnes of four-column hydraulic press, denoted as hot-compressed. The ingots were compressed into a 50 mm in diameter and 118 mm in height cylinder. The thermal pressure is 16 MPa. After hot-compression, some composite samples were heat treated to a T6 condition in two steps: solubilization at 500 °C for 1 h followed by water quenching and then aging at 140 °C for 9 h, denoted as T6. The mechanical properties of this material are listed in Table 1.

### 2.2. Thermal fatigue experiments

The fatigue specimens with 2 mm thick, either as hot-compressed or T6 treated, were cut parallel to the hot-compression direction, then were machined into the shape described in Fig. 1. The two main surfaces of the samples were ground by SiC sandpapers and mechanically-polished to erase the surface scratch. Thus, the

\* Corresponding author. Tel.: +86 731 88821648; fax: +86 731 88821648.  
E-mail address: [lwzzgjajie@126.com](mailto:lwzzgjajie@126.com) (C. Zhenhua).

**Table 1**  
Mechanical properties of the Al–Si/SiC<sub>p</sub> composite.

Composite/condition	Tensile strength (MPa)	Yield strength (MPa)	Elastic modulus (GPa)	Micro-hardness	Density
Hot-compressed	260.0	230	118.7	125.1	2.66
T6	325.0	289.5	126.8	177.8	2.67

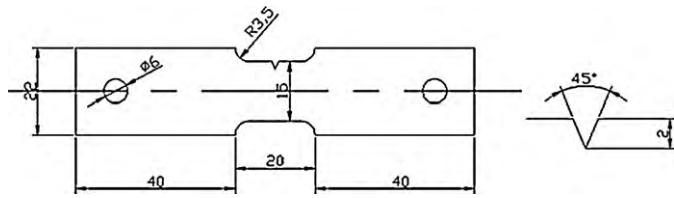


**Fig. 1.** Geometry shape and dimension of the specimen used in thermal fatigue test.

surface quality almost had no effect on the crack initiation and growth in the thermal fatigue tests. Samples of hot-compressed and T6 were submitted to thermal fatigue tests by heating in a furnace with air atmosphere at 450 °C for 15 min and then quenching by free fall into water at 25 °C for 5 seconds. The initiation and propagation of crack from the V-notch root were examined using an optical microscope every 50 thermal cycles, as well as micro-hardness measurements. Microstructure was investigated by scanning electron microscope (SEM) and transmission electron microscopy (TEM). The final porosity of this material after T6 treatment was measured by using water immersion testing when the samples were coated with petroleum jelly.

### 3. Results and discussion

#### 3.1. Fatigue crack shape

Thermal fatigue crack initiation and propagation of specimens have been recorded, as shown in Fig. 2. A thermal fatigue crack is found to initiate from the notch tip, as shown in Fig. 2(a). As can be seen in Fig. 2(b), the crack exhibits deflection and bridging in the propagation stage, which is advantage in improving the thermal fatigue resistance.

#### 3.2. Fatigue crack propagation curve

Fig. 3 shows the variation of crack propagation rate and micro-hardness with the number of thermal cycles for the hot-compressed and T6 samples. It can be seen that crack first appeared in hot-compressed composite, and the crack propagation rate is higher than that of T6 composite. As can be seen in Table 1, after T6 treatment, the micro-hardness and tensile strength values of composite are increased by 42.2% and 25% respectively. Clearly, the differences

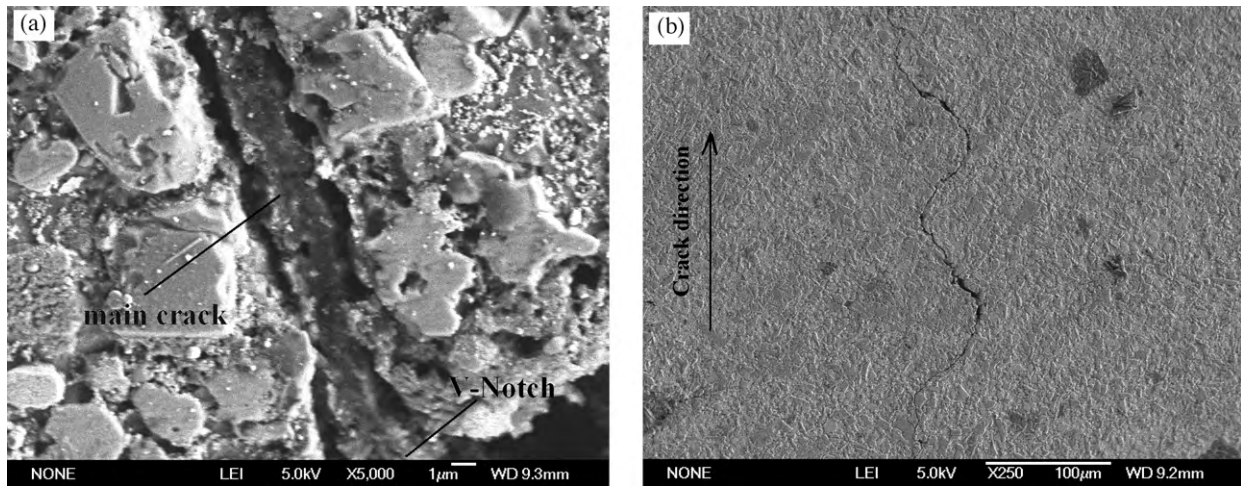


**Fig. 2.** SEM micrographs showing (a) the initiation and (b) propagation of thermal fatigue crack from notch tip in T6 composite.

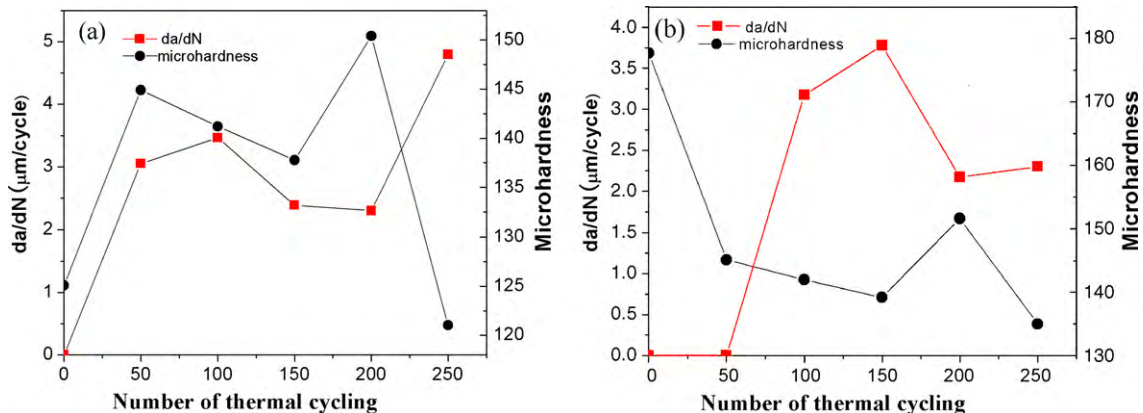


**Fig. 3.** The relationship between crack propagation rate( $da/dN$ ) and micro-hardness after several thermal cycles for the (a) hot-compressed composite and (b) T6 composite.



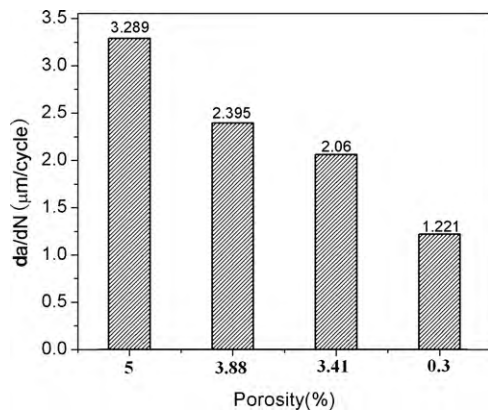


**Fig. 4.** The crack propagation rate ( $da/dN$ ) in T6 composite with different porosity after 200 thermal cycles.

are mainly caused by micro-hardness and strength. Under similar conditions, higher strength and micro-hardness can help to reduce the cyclic plastic strain amplitude caused by thermal stress, thus contributing to inhibiting the occurrence of crack and improving the thermal fatigue resistance of composites.

Furthermore, crack propagation rate and micro-hardness of the both composites exhibit quasi-periodic up-and-down variation since 100 thermal cycles, while exhibiting an opposite variation, i.e. every increase of crack propagation speed corresponds to a decrease of micro-hardness. These characteristics are similar to

those reported in ref. [10]. The up-and-down variation of micro-hardness is related to variations of density of dislocations caused by new stress generation and stress relief, which occur simultaneously during thermal cycling [11–13]. For the present thermal fatigued sample, in the up stage of crack propagation rate, stress relief dominates over stress generation, resulting in relaxation of dislocations, which makes fixed dislocations move anew and cancel each other out, thus decreases both dislocation density and micro-hardness in the material. However, at the peak crack propagation rate, the increase of crack length results in the reduction of local constraint ratio, therefore thermal stress would be relaxed, which leads to the decrease in crack propagation rate. Then, in the down stage of crack propagation rate, an increase of micro-hardness can be observed which results from the increase of dislocation density caused by prevailing new stresses generation. The up-and-down variations of micro-hardness and crack propagation rate indicate that fatigue hardening and fatigue softening occur alternately in the process of thermal fatigue.

However, after the first 50 thermal cycles, the micro-hardness of hot-compressed composite increases from 125.0 to 146.9, while the micro-hardness of the T6 composite decreases from 177.8 to 142.7. It could be considered as aging for the composite with hot-compression and over-aging for the T6 composite in the first 50 thermal cycles.

It is well known that the porosity is an inherent property for the spray-formed composite, although most of them can be eliminated through densification. However, during thermal fatigue test, cracks can be favorably created from these porosities [14]. Therefore, the porosity is a serious microstructural defect and has detrimental

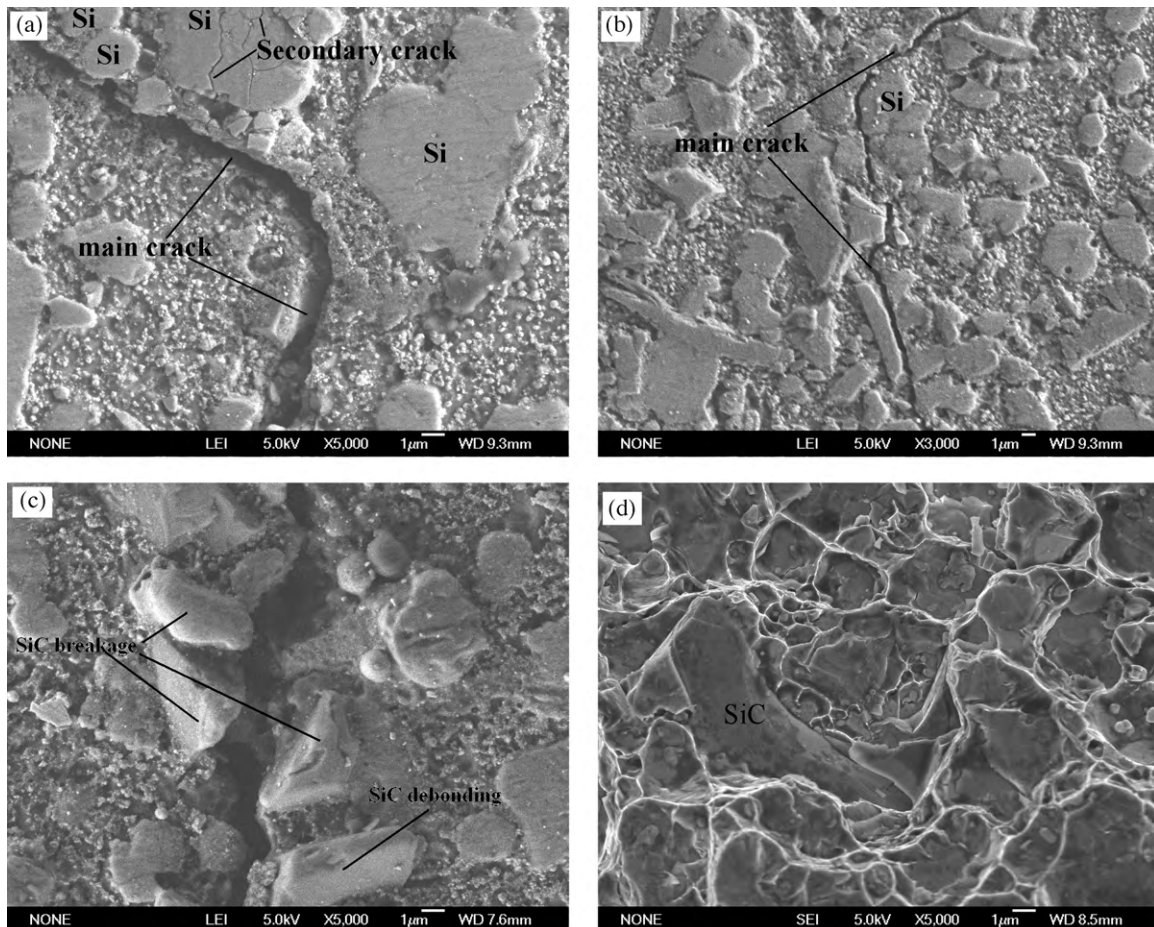


**Fig. 5.** SEM micrograph of thermal fatigue morphology. (a) Propagation of cracking around Si particles; (b) propagation of cracking through large Si; (c) interaction of thermal crack and SiC particles and (d) thermal fatigue fracture surface.

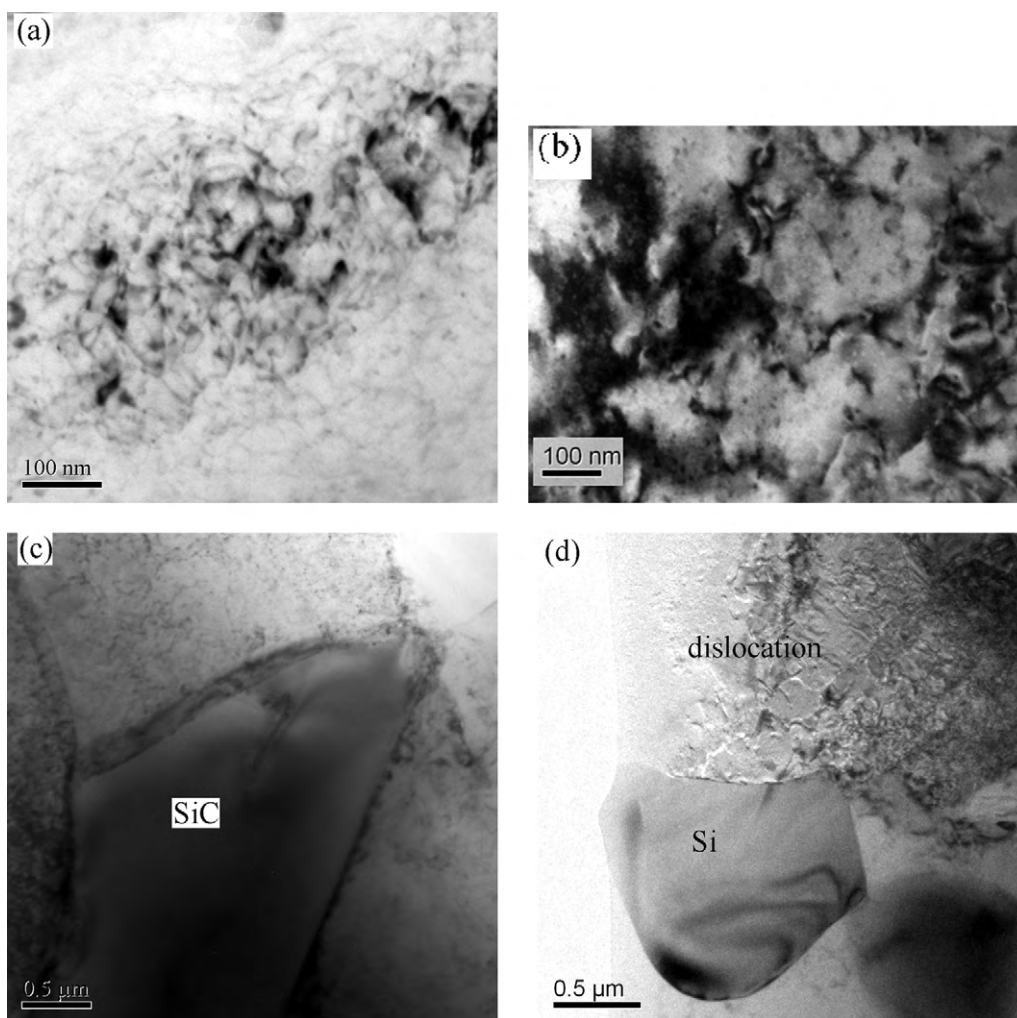


**Fig. 6.** TEM image of composites. (a) Dislocation (T6 treated); (b) high dislocation density (250 thermal cycles); (c) dislocation generated from the SiC sharp corner and (d) interaction of dislocation and Si particles.

influence on the thermal fatigue properties of the material. Fig. 4 shows the crack propagation rate in T6 composite with different porosity. The T6 composite with lower porosity has a significantly smaller crack propagation rate than that with higher porosity and exhibits superior thermal fatigue resistance.

### 3.3. Fatigue crack propagation mechanism

From Fig. 2, path of fatigue crack is seen to alter when the crack tip interacts with the Si and SiC particles. The propagation of thermal fatigue crack is related to the microstructure of Al–Si/SiC<sub>p</sub> composite. Crack propagating through the Si particles (Fig. 5(a)) and around Si particles (Fig. 5(b)) are observed. It is apparent that the crack with an inclination angle to the Si particles  $< 45^\circ$  or  $> 135^\circ$  has a tendency to progress around Si particles, while crack with angles between  $45^\circ$  and  $135^\circ$  is expected to advance through Si particles. There are two ways of the interaction between thermal fatigue crack and SiC particles: SiC particle/matrix debonding and particle breakage (see Fig. 5(c)). A typical debonding of reinforcement/matrix is also observed in the thermal fatigue fracture surface (Fig. 5(d)). Therefore, the resistance of composites to thermal fatigue crack propagation would be improved, by strengthening particle/matrix interface and improving particle quality.

TEM of the composite before and after thermal cycling are compared in Fig. 6. Before cycling, dislocations of the T6 composite

obtain from processing due to the difference in thermal expansion coefficient between the aluminum matrix and the reinforcement are present in Fig. 6(a). Thermal cycling causes quantities of the sources of dislocation multiplication and movement tendency of dislocations under the thermal stress and thermally misfit stress loading (see Fig. 6(b)). The dislocation interaction during thermal cycling can increase dislocation density, resulting in the cyclic hardening behavior of the composite. Moreover, the SiC sharp corner is able to emit dislocations during thermal cycling, this could turn the trend of dislocation density becoming higher (Fig. 6(c)). However, the dispersed particulate like Si phase plays a role of hindrance for the dislocation movement (Fig. 6(d)). Then, it also increases the resistance for the plastic deformation.

## 4. Conclusions

The following conclusions could be made based on the results of thermal fatigue tests and subsequent microstructural analysis:

- (1) Samples with high micro-hardness, low porosity volume fraction show superior thermal fatigue resistance.
- (2) Fatigue crack propagation rate and micro-hardness exhibit quasi-periodic up-and-down variations with an increase in the number of fatigue cycles. The variations result from variations of dislocation density caused by new stresses generation and

stress relief dominating alternately. It indicates that fatigue hardening and fatigue softening occur alternately in the process of thermal fatigue.

- (3) Crack propagating through and around Si particles are observed. The cracking of SiC particles and the debonding of reinforcement/matrix are proven to be the main mechanism when the crack-tip interacts with SiC particles. Thermal cycling caused quantities of the sources of dislocation multiplication and movement tendency of dislocations.

#### Acknowledgement

The authors are grateful to the international cooperation of Hunan Province in China (project 2007WK2005) for the support of the present research.

#### References

- [1] P. Rohatgi, JOM 43 (1991) 10–15.
- [2] H. Nakanishi, K. Kakihara, A. Nakayama, T. Murayama, JSAE Rev. 23 (2002) 365–370.
- [3] A.R.E. Singer, Met. Matter. 4 (1970) 246.
- [4] W.C. Revelos, J.W. Jones, E.J. Dolley, Metall. Mater. Trans. A 26 (1995) 1167–1181.
- [5] N.N.V. Prasad, M.H. Aliabadi, D.P. Rooke, Int. J. Fatigue 18 (1996) 349–361.
- [6] A.E. Herr, S. Canumalla, R.N. Pangborn, Mater. Sci. Eng. 200 (1995) 181–191.
- [7] W.C.M. Lawrence, G.W. Han, Composites 37 (2006) 1858–1862.
- [8] E. Ghorbel, Comp. Sci. Technol. 57 (1997) 1045–1056.
- [9] C. Zhenhua, Multi-Layer Spray Deposition Technology Applications, 1st ed., Hunan University Publications, Chinese, 2003.
- [10] C.Q. Tang, G.Y. Li, Z.H. Shi, Aust. J. Phys. 53 (2000) 829–834.
- [11] F.S. Shieu, S.L. Sass, Acta Metall. Mater. 39 (1991) 539–547.
- [12] S.M. Pickard, B. Derby, Acta Metall. Mater. 38 (1990) 2537–2552.
- [13] S.L. Hong, G.T. Gray III, K.S. Vecchio, Mater. Sci. Eng. A171 (1993) 181–189.
- [14] J.Y. Buffiere, S. Savelli, P.H. Jouneau, Mater. Sci. Eng. A 316 (2001) 115–126.